Title
Rapid differentiation of the human RPE cell line, ARPE-19, induced by nicotinamide

Authors
Hazim, Roni A
Volland, Stefanie
Yen, Alice
et al.

Publication Date
2019-02-01

DOI
10.1016/j.exer.2018.10.009

Peer reviewed

HHS Public Access

Author manuscript

Exp Eye Res. Author manuscript; available in PMC 2020 February 01.

Published in final edited form as:

Exp Eye Res. 2019 February ; 179: 18–24. doi:10.1016/j.exer.2018.10.009.

Rapid differentiation of the human RPE cell line, ARPE-19, induced by nicotinamide

Roni A. Hazim[a], **Stefanie Volland**[a], **Alice Yen**[a], **Barry L. Burgess**[a], **David S. Williams**[a,b,c,d,*]

[a]Department of Ophthalmology and Stein Eye Institute, David Geffen School of Medicine at UCLA

[b]Department of Neurobiology, David Geffen School of Medicine at UCLA

[c]Molecular Biology Institute, University of California, Los Angeles, CA

[d]Brain Research Institute, University of California, Los Angeles, CA

Abstract

Human RPE cell lines, especially the ARPE-19 cell line, are widely-used in eye research, as well as general epithelial cell studies. In comparison with primary RPE cells, they offer relative convenience and consistency, but cultures derived from these lines are typically not well differentiated. We describe a simple, rapid method to establish cultures from ARPE-19 cells, with significantly improved epithelial cell morphology and cytoskeletal organization, and RPE-related functions. We identify the presence of nicotinamide, a member of the vitamin B family, as an essential factor in promoting the observed differentiation, indicating the importance of metabolism in RPE cell differentiation.

1. Introduction

The retinal pigment epithelium (RPE) is a single monolayer of cells that resides between the light-sensitive photoreceptors and the fenestrated choriocapillaris. It performs specific functions in support of the photoreceptor cells, including the reisomerization of visual chromophore, and phagocytosis of photoreceptor outer segment (POS) membrane (Strauss, 2005). The importance of the RPE for proper vision is underscored by several retinal degenerative diseases that involve RPE pathology, including age-related macular degeneration (AMD) (Bhutto and Lutty, 2012).

Due to the scarcity of donor eyes, primary human RPE cells are in limited supply. Moreover, these primary cultures exhibit significant heterogeneity among cultures from different donors (Burke et al., 1996; Kuznetsova et al., 2014). In addition to donor eyes, human RPE

*Corresponding author: David S. Williams, Stein Eye Institute, David Geffen School of Medicine at UCLA, 100 Stein Plaza, Los Angeles, CA 90095, dswilliams@ucla.edu.

Author Contributions

R.A.H. and D.S.W. designed research, analyzed data, and wrote the manuscript. R.A.H., S.V. and A.Y. performed research. B.L.B. analyzed data.

cells can be derived from embryonic and induced pluripotent stem cells (Idelson et al., 2009; Buchholz et al., 2013; Hazim et al., 2017). Although the RPE cells differentiated from stem cells have been shown to exhibit native RPE characteristics, the differentiation process is costly and time-consuming. Furthermore, stem cell-derived RPE cells have been found to lose their polarized organization and RPE functions after only a few passages in culture (Singh et al., 2013). Hence, human RPE cell lines continue to provide an important source, with the ARPE-19 line being the most commonly used; in recent years, there have been ~170 papers published annually that specifically mention ARPE-19 cells in the title or abstract (PubMed search for ARPE-19 or ARPE19).

When first reported, standard cultures of the ARPE-19 cell line readily exhibited many of the characteristics of well-differentiated RPE cells, including cobblestone morphology, apical-basal polarity, and expression of RPE-specific proteins (Dunn et al., 1996). However, after two decades of passaging, such well-differentiated cultures no longer form with the commonly-used culture methods. The cells typically exhibit incomplete execution of the epithelial polarity program (Rodriguez-Boulan and Macara, 2014), thus compromising their ability to represent *in vivo* biology. We describe here a significantly-improved method to culture ARPE-19 cells that are currently commercially available. It involves culture in medium with supplements including nicotinamide (referred to as MEM-Nic hereafter), and selective trypsinization to generate a homogeneous cell population. The requirement for nicotinamide demonstrates the importance of metabolism in differentiation of the cells.

2. Materials and supplies

2.1 Cell culture components

Dulbecco's Modified Eagle Medium (DMEM)/F12 with GlutaMAX, Minimum Essential Medium (MEM) Alpha, certified-grade fetal bovine serum (FBS; US origin), nonessential amino acids (NEAA), TrypLE Express Enzyme (1X), and Penicillin/Streptomycin were obtained from Thermo Fisher Scientific (Waltham, MA). The N1 supplement, taurine, hydrocortisone, triiodothyronin, and nicotinamide were obtained from Sigma-Aldrich (St. Louis, MO). ARPE-19 cells were obtained from ATCC (Lot Number 63478793; Manassas, VA) at their currently advertised passage number of 19, cultured on T75 flasks or 6-well tissue culture plates, and differentiated on Transwell inserts with polyester membrane (6.5-mm diameter, 0.4-μm pores) from Corning Costar (St. Louis, MO), and coated with natural mouse laminin (Thermo Fisher Scientific).

2.2 Antibodies

The primary antibodies used for immunocytochemistry included: rabbit anti-ZO-1 (Invitrogen 402200), rabbit anti-OCLN (Abcam ab31721), mouse anti-BEST1 (Abcam ab2182), mouse anti-α-tubulin (Sigma-Aldrich T9026), 4D2 mouse anti-opsin (Millipore MABN15), rabbit anti-PEDF (BioProducts MD AB-PEDF1), and mouse anti-acetylated α-tubulin (Sigma-Aldrich T6793). The secondary antibodies used were goat anti-mouse and goat anti-rabbit IgG conjugated to Alexa Fluor 488 or 594 (Life Technologies). For western blotting, the antibodies used included: rabbit anti-RPE65 (pin 5) (Wenzel et al., 2005) (gift from Andreas Wenzel) and goat anti-FH (Quidel A312).

2.3 RT-PCR Primers

For RT-PCR, the sequences of primers used include: *RPE65*, 5' – GATCTCTGCTGCTGGAAAGG – 3' and 5' – TGGGGAGCGTGACTAAATTC – 3'; *BEST1*, 5' – CCCGAAAATCACCTCAAAGA – 3' and 5' - GCTTCATCCCTGTTTTCCAA – 3'; *OCLN*, 5' – GGAGGACTGGATCAGGGAAT – 3' and 5' – TCAGCAGCAGCCATGTACTC – 3'; *MERTK*, 5' – AGACTTCAGCCACCCAAATG – 3' and 5' – GGGCAATATCCACCATGAAC – 3'; and *ITGB5*, 5' – CGGGGACAACTGTAACTGCT – 3' and 5' – ACGCAATCTCTCTTGGTGCT – 3'.

The primers used for *BEST1*, *OCLN*, and *ITGB5* span exon-exon junctions as to avoid amplification of genomic DNA. The primers used for *RPE65* and *MERTK* could theoretically generate products from genomic DNA. However, this is unlikely, given that such amplicons would be larger than 7 kb.

3. Detailed methods

3.1 Cobblestone morphology

ARPE-19 were thawed and cultured in DMEM/F12 with GlutaMAX, 10% certified FBS, and 1% Penicillin/Streptomycin until the culture vessel was 95–100% confluent. For medium comparison studies, the cells were passaged and cultured in a 6-well tissue culture plate (seeding density, 1.66×10^5 cells.cm^{-2}) or on a Transwell filter insert (at the same density) in one of the following media: **(1) DMEM/F12** (DMEM/F12, 1% FBS, and 1% Penicillin/Streptomycin); **(2) DMEM + pyruvate** (DMEM with high glucose (4.5 g/l), 1 mM pyruvate, and 1% Penicillin/Streptomycin); **(3) MEM-Nic** (MEM alpha with GlutaMAX, 1% FBS, 1% Penicillin/Streptomycin, 1% N1 supplement, taurine (0.25 mg/ml), hydrocortisone (20 ng/ml), triiodo-thyronin (0.013 ng/ml), and 10 mM nicotinamide). The cells were maintained at 37°C, 5% CO_2, and the media were replaced with fresh media three times per week.

First, we examined the gross morphology of ARPE-19 cells in two standard media commonly used to culture these cells and compared them with those cultured in MEM-Nic. As a simple epithelium, RPE forms a single monolayer with cobblestone appearance. After one week in culture on a plastic tissue culture plate, with either of the standard media, the ARPE-19 cells appeared elongated, lacking epithelial organization, as evident by bright-field microscopy. In contrast, the cells cultured in MEM-Nic formed a monolayer of mostly epithelial-like cells, exhibiting cobblestone morphology (Fig. 1A). When grown on Transwell inserts (as described in the next section) for one week, and examined by immunofluorescence of zona occludens-1 (ZO-1), which labels the periphery of the cells, a comparable difference was evident (Fig. 1B). After an extended period in culture, we observed improvements in the organization of ARPE-19 cultures in the two standard media, with the appearance of a cobblestone-like morphology after ~2 months, but still not to the extent of cells after one week in culture with MEM-Nic.

3.2 Role of nicotinamide in ARPE-19 cell differentiation

Given the role that nicotinamide has been shown to play in the differentiation of RPE from pluripotent stem cells (Idelson et al., 2009; Maruotti et al., 2015; Saini et al., 2017), we tested the necessity of nicotinamide in the MEM-Nic medium for the observed morphological phenotype. We thus compared cultured ARPE-19 cells in the presence or absence of nicotinamide, or a nicotinamide-related compound, nicotinamide riboside (NR). Brightfield micrographs revealed that, in MEM-Nic without nicotinamide (but with the other supplements), the cells failed to acquire cobblestone morphology. They also showed that the addition of 10 mM NR was approximately as effective as 10 mM nicotinamide in inducing the rapid differentiation of ARPE-19 cells (Fig. 1C). The cobblestone arrangement of ARPE-19 cultures, grown on Transwell inserts in MEM with 10 mM Nic or 10 mM NR, is evident by ZO-1 immunofluorescence (Fig. 1C, right panels).

As a member of the vitamin B3 family, nicotinamide has been implicated to play a central role in cellular metabolism. In particular, it serves as a precursor for the production of NAD^+, $NADP^+$, and other substrates that participate in metabolic pathways, including the TCA cycle, and the mitochondrial electron transport chain (Jang et al., 2012). Interestingly, many of the key enzymes and coenzymes in these metabolic pathways have been shown to become upregulated as cells differentiate into their terminal fate (Shyh-Chang et al., 2013; Hu et al., 2016). Nicotinamide has been shown to protect against oxidative stress and maintain mitochondrial health (Gomes et al., 2013; Mitchell et al., 2018), while its related compound, NR, was demonstrated to promote oxidative metabolism by means of increasing the NAD^+/NADH ratio (Canto et al., 2012). Interestingly, there is evidence to suggest that oxidative stress, and in particular reactive oxygen species, can promote epithelial-to-mesenchymal transition (Rhyu et al., 2005; Wang et al., 2010).

3.3 Culture on permeable Transwell inserts

Transwell culture systems provide a permeable support for epithelial cells that promotes their differentiation *in vitro* into a polarized state by establishing distinct apical and basal compartments. To generate homogenous polarized monolayers, ARPE-19 cells differentiated in MEM-Nic for two weeks in plastic vessels were subjected to three 10-minute treatments with TrypLE, a recombinant trypsin substitute. The TrypLE was discarded after each 10-min treatment, releasing weakly-adherent fibroblastic-like cells (representing ~5% of cells in the cultures), leaving behind the firmly attached epithelial cells. This method of selective trypsinization generates a homogenous population of cobblestone cells in subsequent cultures. Following the last treatment of TrypLE, the remaining cells were harvested in MEM-Nic (by gentle pipetting) and the suspension was passed through a 40-μm cell strainer (BD Falcon) to ensure the absence of cell clumps. Cells were then counted on a hemocytometer and plated on laminin-coated (10 $\mu g.cm^{-2}$) Transwell inserts at a density of 1.66×10^5 $cells.cm^{-2}$ in MEM-Nic. The 100 μl of medium in the apical compartment and the 600 μl in the basal compartment of each Transwell insert were replaced with fresh medium three times per week.

3.4 Characterization of the apical microvilli and the cytoskeleton

Differentiated ARPE-19 cells grown on Transwells were prepared for transmission electron microscopy (TEM), and fixed by removing the culture medium and replacing it with primary fixative, 2% formaldehyde and 2.5% glutaraldehyde (EM grade from Electron Microscopic Sciences) in 0.1 M sodium cacodylate buffer. After 20 min fixation, the Transwell membrane was excised with a scalpel, washed with 0.1 M sodium cacodylate buffer and osmicated for 20 min with 1% osmium tetroxide in 0.1 M sodium cacodylate buffer. Samples were then dehydrated in an ethanol series, washed with propylene oxide, and embedded in Araldite 502 resin (Electron Microscopic Sciences, Hatfield, USA). Ultrathin sections were collected on copper mesh grids and contrast-stained with 5% uranyl acetate in ethanol and 0.4% lead citrate.

For immunofluorescence, cells cultured on Transwell inserts were washed twice with Dulbecco's phosphate buffered saline (DPBS; Fisher Scientific), and fixed with 4% formaldehyde in DPBS for 10 min. Following 3 washes with DPBS, the cells were permeabilized with 0.25% Triton X-100, and then blocked in DPBS containing 5% normal goat serum and 1% BSA for 1 h. The cells were then incubated for 1 h at RT in DPBS containing 1% BSA and one or a combination of primary antibodies. Following the primary-antibody incubation, the cells were washed 3×5 min, and incubated with appropriate Alexa Fluor-conjugated secondary antibodies and, in some instances, Phalloidin-TRITC (Sigma-Aldrich) for 1 h at RT in the dark. The cells were washed 3×5 min with DPBS, and the membranes of the Transwell inserts were excised and mounted on microscope slides using Fluoro-Gel II mounting medium with DAPI (Electron Microscopy Sciences) to counterstain the nuclei. Images were acquired on a confocal microscope (FluoView 1000, Olympus) with FluoView FV10-ASW 3.1 software.

Electron microscopy revealed the presence of microvilli emanating from the apical surface of differentiated ARPE-19 cells (Fig. 1D). Fluorescence microscopy demonstrated an epithelial-like arrangement of cytoskeletal elements. Phalloidin labeling revealed actin filaments in the apical RPE, with a circumferential ring at the level of the cell-cell junctions (Fig. 1E). By immunolabeling, we also observed that apically-located microtubules were horizontal (Fig. 1F) while those found more basally were vertically-oriented (Fig. 1G). In addition to these classes of microtubules, immunolabeling with antibodies specific for acetylated α-tubulin indicated the presence of cilia at the apical surface of the cells (Supplementary Fig. 1).

Because these cytoskeletal elements support actin-based (myosins) and microtubule-based (dyneins and kinesins) motility, they play an essential role in organelle trafficking and protein sorting. In epithelial cells, the spatial organization of microtubules, in addition to their associated motors, have been shown to be critical for the polarized targeting of secretory vesicles, as well as the machinery of the endocytic pathway (Gilbert et al., 1991; Musch, 2004). The ARPE-19 cells differentiated by our method establish a polarized epithelial cell model that can be used to investigate general epithelial processes, including secretory and endocytic vesicular transport, as well as RPE-specific processes such as the trafficking of phagosomes and the degradative organelles that are necessary for their clearance (Wavre-Shapton et al., 2014; Jiang et al., 2015; Esteve-Rudd et al., 2018).

3.5 Expression of RPE genes

Total RNA was harvested from ARPE-19 cells differentiated on plastic for 2 weeks using Qiagen RNeasy Plus Mini Kit (cat # 74134) following the manufacturer's protocol. Single-strand cDNA was synthesized from 2 μg of total RNA using the SuperScript III First-Strand Synthesis Kit (Invitrogen). PCR was performed using Taq PCR Premix (Bioland Scientific). Thermal cycling conditions were as follows: one cycle at 95 °C for 5 min; 40 cycles at 95 °C for 15 s, 60 °C for 15 s, and 72 °C for 20 s; and one cycle at 72 °C for 5 min.

To test for the expression of RPE-signature genes, we probed for *RPE65*, encoding an essential retinoid isomerase required for the visual cycle function, bestrophin 1 (*BEST1*), encoding an RPE-specific protein localized to the basolateral surface, occludin (*OCLN*), encoding a tight junction component, and *MERTK* and integrin β5 (*ITGB5*), encoding critical receptors for the phagocytosis of photoreceptor outer segment disk membranes. RT-PCR revealed that two-week cultures of ARPE-19 cells in MEM-Nic detected the expression of all these genes (Fig. 2A).

3.6 Protein expression, localization, and secretion

SDS-PAGE was performed to separate 20 ug of proteins (denatured at 95 °C for 5 min) from whole-cell lysates on a 4–12% bis-tris gradient gel. Proteins were transferred onto PVDF membrane using semi-dry transfer. Membranes were blocked with Odyssey blocking buffer (LICOR) for 1 h at RT to prevent non-specific binding of the antibodies. For RPE65 detection, the membrane was incubated with rabbit anti-RPE65 (pin 5) in Odyssey buffer containing 0.1% Tween-20 overnight at 4 °C. The signal was detected by incubating the membrane with goat anti-rabbit IRDye 800CW secondary antibodies in Odyssey buffer with 0.1% Tween-20 and 0.01% SDS for 1 h at RT. For Factor H detection in ARPE-19 conditioned medium, samples were collected from the apical and basal compartments of Transwell inserts (six times more volume was collected from the basal compartment relative to the apical compartment to account for the medium volumes used when culturing the cells). The samples were heated at 70 °C for 10 min before being separated on a 4–12% bis-tris gradient gel. The transfer and blocking steps were performed as described above. The membrane was incubated with goat anti-FH for 2 h at RT followed by an incubation with donkey anti-goat IRDye 800CW secondary antibodies. Blots were imaged using the Odyssey CLx Imaging System (LI-COR) and processed using Image Studio Lite Ver5.2 software.

Western blotting confirmed the expression of RPE65 protein (Fig. 2B; Supplementary Fig. 2A). After 3 weeks of differentiation, properly localized OCLN (Fig. 2C) and BEST1 (Fig. 2D), were detected at the apical and basolateral surfaces, respectively. Taken together, these data show that ARPE-19 cells can be rapidly differentiated such that their expression of some key RPE proteins compares to native RPE.

Demonstration of polarity in differentiated ARPE-19 cells was evident in the vectorial secretion of complement factor H. The RPE is a local source of Factor H in the retina, and the gene (*CFH*) is one of the two very high-risk genes for AMD (Edwards et al., 2005; Haines et al., 2005). Serum-free media conditioned by ARPE-19 cells differentiated on

Transwell inserts for 48 h was collected from the apical and basal compartments of the inserts and tested for Factor H using western blotting. The results demonstrated significantly more Factor H present in the apical medium relative to the basal medium (Fig. 2E; Supplementary Fig. 2B), suggesting that the protein is secreted in a polarized manner, similar to that observed in vivo. This observation is consistent with immunofluorescence data showing Factor H localization on the apical surface of human fetal RPE cultured on Transwell inserts (Kim et al., 2009). Additional demonstration of polarity in differentiated ARPE-19 cells was evident in the apical localization of the pigment epithelium-derived factor (PEDF) (Fig. 2F), a protein known to be secreted from the apical surface of polarized RPE cells (Tombran-Tink et al., 1995).

3.7 Phagocytosis of photoreceptor outer segments and degradation of phagosomes

To test the functionality of differentiated ARPE-19 cells, we focused on an essential function of the RPE, phagocytosis of POSs. To prepare isolated POSs, fresh porcine eyes were obtained from a local slaughterhouse and kept on ice at all times. POSs were isolated using a previously published protocol for isolation of bovine POSs (Azarian et al., 1995), with a few modifications. Briefly, the retinas were isolated from eyecups under dim red light and homogenized with a Teflon glass pestle. The homogenate was then loaded onto a continuous (27–50%) sucrose gradient and centrifuged at 26,000 *g* for 1 h at 4 °C. Following centrifugation, the POSs settle in a band on the gradient, easily identifiable due to its orange/pink color. The band containing the POSs was collected, diluted three times in Ringer solution (130 mM NaCl, 3.6 mM KCl, 2.4 mM $MgCl_2$, 1.2 mM $CaCl_2$, 10 mM HEPES, and 0.02 mM EDTA, pH 7.4) and centrifuged at 10,000 *g* for 10 min at 4 °C. The POSs were counted under a hemocytometer and stored in DMEM with 2.5% sucrose at −80 °C for subsequent experiments. POSs were stored frozen. Immediately prior to use they were thawed at RT and centrifuged at 2,400 *g* for 5 min. The POSs were then suspended in DMEM, and FBS was added at 10% final concentration.

ARPE-19 cells, cultured on Transwell inserts in MEM or MEM-Nic, were then challenged with 100 μl of POS suspension (~7.5×10^7 POSs/ml) for 2 h at 37 °C, 5% CO_2. After the POS challenge, cells were extensively washed with DPBS containing 0.9 mM calcium and 0.5 mM magnesium (DPBS-CM), and immediately processed for immunofluorescence (pulse) or returned to the 37 °C incubator for 1 h (chase) before being processed for immunofluorescence. A previously described double immunofluorescence labeling strategy (Hazim and Williams, 2018) was used to distinguish between POSs bound to the surface of the ARPE-19 cells and POSs that have been internalized (Fig. 3A). Briefly, the cells were fixed with 4% formaldehyde (Electron Microscopy Sciences) for 10 min and blocked with blocking buffer (1% BSA in DPBS-CM) for 15 min. Surface-bound POSs were then labeled with the 4D2 mouse anti-opsin antibodies diluted in blocking buffer for 10 min, followed by an Alexa Fluor 488 nm-conjugated donkey anti-mouse secondary antibodies for 30 min, in the dark. The cells were then permeabilized with 50% ethanol for 10 min at RT. All POSs were then labeled with the same opsin antibody followed by an Alexa Fluor 594 nm-conjugated donkey anti-mouse secondary antibody for 1 h at RT. Finally, cells were washed with DPBS-CM before the membranes of the Transwell inserts were excised and mounted on to frosted microscope slides using Fluoro-Gel II mounting medium with DAPI. Confocal

Z-stacks of ≥ 4 randomly selected fields of view were acquired on an Olympus confocal microscope.

Surface-bound POSs were labeled with both secondary antibodies, thereby appearing yellow in color. The internalized POSs were labeled post-cell permeabilization with the Alexa Fluor 594 nm-conjugated secondary antibody and therefore appear red in color (Fig. 3A). Quantification of opsin-positive particles after a 2-h exposure to POSs (pulse), and then after an additional 1 h (chase), following the removal of the POSs by washing, was performed to compare the rates of POS ingestion and POS phagosome degradation by ARPE-19 cells in MEM and in MEM-Nic (Fig. 3B).

Cells cultured in either medium had POSs bound to their surface following the 2-h pulse. Those cultured in MEM-Nic had fewer bound POSs, consistent with other studies. In primary rat RPE cultures, it was shown that densely packed cells required longer incubation periods to bind POSs, but ingested them in a more rapid and synchronized manner than highly spread cells (McLaren, 1996). Human primary RPE cells that were differentiated, showing epithelial morphology, exhibited less binding of POSs when compared with cells that were less differentiated. This observation was attributed to fewer alphaV-beta5 integrin receptors on the surface of the more differentiated cells (Miceli et al., 1997). The more extensive apical microvilli of differentiated cells may also retard access to the receptors in cell culture assays.

Determination of the number of internalized POSs (≥ 1 μm in diameter), relative to the total number of POSs, showed that cells cultured in MEM-Nic had relatively more internalized POSs, indicating more rapid ingestion. The ingestion rate in MEM-Nic is likely to have been even greater than that indicated by counting internalized POSs, since the degradation rate was also greater. Comparison of the total number of POSs, following the 1-h chase, showed that less than 30% of the POSs remained in MEM-Nic cells, whereas the cells in MEM without nicotinamide showed no significant reduction in POS number (Fig. 3B). Therefore, although the ARPE-19 cells with cobblestone morphology have lower POS binding capabilities, they ingest the bound POSs and degrade the POS phagosomes with more rapid kinetics.

4. Limitations

4.1 Low trans-epithelial resistance in differentiated ARPE-19 cells

Trans-epithelial resistance (TER), a measure of the barrier function of an epithelium, was measured for differentiated ARPE-19 cells cultured on laminin-coated Transwell inserts using an EVOM^2 Epithelial Voltohmmeter (World Precision Instruments) with an STX2 electrode, as described previously for RPE cell cultures from iPS cells (Hazim et al., 2017). All measurements were made inside a biosafety cabinet within 3 minutes of cell removal from the incubator. The net TER was determined by subtracting the resistance across a laminin-coated Transwell insert without any cells from measured values, and multiplying by the growth surface of the Transwell insert (0.33 cm^2).

In comparison to RPE cells in vivo or primary culture, ARPE-19 cell cultures have invariably been reported to possess a relatively low TER. Even with the original ARPE-19 cultures, Dunn et al. (Dunn et al., 1996) reported TER values of 34 Ohms.cm^2 in DMEM/F12 medium. In DMEM-Pyruvate, a TER of 51 Ohms.cm^2 was reported (Ahmado et al., 2011). In MEM-Nic, we measured 40 Ohms.cm^2 after 6 weeks, which is comparable to these published values and still relatively low.

4.2 Lack of pigmentation

Although the premelanosome marker, Pmel17, has been detected in ARPE-19 cells (Ahmado et al., 2011), images of normal RPE melanosomes have never been shown. Nonetheless, a lack of pigmentation is usually considered an advantage when working with fluorescence, which is readily quenched by melanin (especially the shorter wavelengths).

4.3 Abnormal karyotype

The immortalization of the ARPE-19 cell line occurred spontaneously, and in a recent study (Fasler-Kan et al., 2018), it was shown that different sources of the cell line exhibited abnormal karyotypes. Interestingly, attempts by these researchers to generate clonal lines with normal karyotype failed because those cells undergo cellular senescence. To test for major chromosomal aberrations in ARPE-19 cells used in this study, cells (p17) were passaged onto a T-25 flask at 50–70% confluency, and shipped to Cell Line Genetics for karyotyping.

Cytogenetic analysis of 20 G-banded metaphase cells revealed an abnormal karyotype, most notably, a loss of one copy of chromosome 15, and an unbalanced translocation between the chromosome 15q and 19q (Supplementary Fig. 3). The karyotype of our cells was similar to that reported by Fasler-Kan et. al. (2018). Despite these chromosomal aberrations, our study shows that the cells can still be differentiated into an RPE-like state.

5. Concluding comment

MEM-Nic cultures of ARPE-19 cells should be particularly useful for studies of RPE intracellular events, where it is essential to have properly polarized cells. For example, studies of many cellular processes, such as organelle transport, depend on the organization of the cytoskeleton, which undergoes major changes during epithelial cell differentiation. Studies of these events are important for understanding many RPE functions and retinal pathologies. So far, two other RPE laboratories have tested the described protocol, and, in preliminary studies, report an improvement in the rate and extent of ARPE-19 cell differentiation over other methods (Drs Kathleen Boeze-Battaglia (University of Pennsylvania) and Stephen Moss (University College London), personal communication).

Supplementary Material

Refer to Web version on PubMed Central for supplementary material.

Acknowledgements

The study was supported by National Institutes of Health Grants F31EY026805 (R.A.H), R01EY013408, R01EY027442 (D.S.W) and P30EY0331. The authors declare no competing interests.

Abbreviations

AMD	age-related macular degeneration
BEST1	bestrophin 1
CFH	complement factor H
ITGB5	integrin β5
FH	factor H
NR	nicotinamide riboside
OCLN	occludin
PEDF	pigment epithelium-derived factor
POS	photoreceptor outer segment
RPE	retinal pigment epithelium
TER	transepithelial resistance
ZO-1	zona occludens-1

References

Ahmado A, Carr AJ, Vugler AA, Semo M, Gias C, Lawrence JM, Chen LL, Chen FK, Turowski P, da Cruz L, and Coffey PJ 2011 Induction of differentiation by pyruvate and DMEM in the human retinal pigment epithelium cell line ARPE-19. Invest Ophthalmol Vis Sci. 52:7148–7159. [PubMed: 21743014]

Azarian SM, King AJ, Hallett MA, and Williams DS 1995 Selective proteolysis of arrestin by calpain. Molecular characteristics and its effect on rhodopsin dephosphorylation. J Biol Chem. 270:24375–24384. [PubMed: 7592650]

Bhutto I, and Lutty G 2012 Understanding age-related macular degeneration (AMD): relationships between the photoreceptor/retinal pigment epithelium/Bruch's membrane/choriocapillaris complex. Mol Aspects Med. 33:295–317. [PubMed: 22542780]

Buchholz DE, Pennington BO, Croze RH, Hinman CR, Coffey PJ, and Clegg DO 2013 Rapid and efficient directed differentiation of human pluripotent stem cells into retinal pigmented epithelium. Stem Cells Transl Med. 2:384–393. [PubMed: 23599499]

Burke JM, Skumatz CMB, Irving PE, and McKay BS 1996 Phenotypic heterogeneity of retinal pigment epithelial cells in vitro and in situ. Exp Eye Res. 62:63–73. [PubMed: 8674514]

Canto C, Houtkooper RH, Pirinen E, Youn DY, Oosterveer MH, Cen Y, FernandezMarcos PJ, Yamamoto H, Andreux PA, Cettour-Rose P, Gademann K, Rinsch C, Schoonjans K, Sauve AA, and Auwerx J 2012 The NAD(+) precursor nicotinamide riboside enhances oxidative metabolism and protects against high-fat diet-induced obesity. Cell Metab. 15:838–847. [PubMed: 22682224]

Dunn KC, Aotaki-Keen AE, Putkey FR, and Hjelmeland LM 1996 ARPE-19, A Human Retinal Pigment Epithelial Cell Line with Differentiated Properties. Exp. Eye Res. 62:155160.

Edwards AO, Ritter R 3rd, Abel KJ, Manning A, Panhuysen C, and Farrer LA 2005 Complement factor H polymorphism and age-related macular degeneration. Science. 308:421–424. [PubMed: 15761121]

Esteve-Rudd J, Hazim RA, Diemer T, Paniagua AE, Volland S, Umapathy A, and Williams DS 2018 Defective phagosome motility and degradation in cell nonautonomous RPE pathogenesis of a dominant macular degeneration. Proc Natl Acad Sci U S A. 115:5468–5473. [PubMed: 29735674]

Fasler-Kan E, Aliu N, Wunderlich K, Ketterer S, Ruggiero S, Berger S, and Meyer P 2018 The Retinal Pigment Epithelial Cell Line (ARPE-19) Displays Mosaic Structural Chromosomal Aberrations. Methods Mol Biol. 1745:305–314. [PubMed: 29476476]

Gilbert T, Le Bivic A, Quaroni A, and Rodriguez-Boulan E 1991 Microtubular organization and its involvement in the biogenetic pathways of plasma membrane proteins in Caco-2 intestinal epithelial cells. J Cell Biol. 113:275–288. [PubMed: 1672691]

Gomes AP, Price NL, Ling AJ, Moslehi JJ, Montgomery MK, Rajman L, White JP, Teodoro JS, Wrann CD, Hubbard BP, Mercken EM, Palmeira CM, de Cabo R, Rolo AP, Turner N, Bell EL, and Sinclair DA 2013 Declining NAD(+) induces a pseudohypoxic state disrupting nuclear-mitochondrial communication during aging. Cell. 155:1624–1638. [PubMed: 24360282]

Haines JL, Hauser MA, Schmidt S, Scott WK, Olson LM, Gallins P, Spencer KL, Kwan SY, Noureddine M, Gilbert JR, Schnetz-Boutaud N, Agarwal A, Postel EA, and Pericak-Vance MA 2005 Complement factor H variant increases the risk of age-related macular degeneration. Science. 308:419–421. [PubMed: 15761120]

Hazim RA, Karumbayaram S, Jiang M, Dimashkie A, Lopes VS, Li D, Burgess BL, Vijayaraj P, Alva-Ornelas JA, Zack JA, Kohn DB, Gomperts BN, Pyle AD, Lowry WE, and Williams DS 2017 Differentiation of RPE cells from integration-free iPS cells and their cell biological characterization. Stem Cell Research & Therapy. 8:1–17. [PubMed: 28057078]

Hazim RA, and Williams DS 2018 Cell Culture Analysis of the Phagocytosis of Photoreceptor Outer Segments by Primary Mouse RPE Cells. Methods Mol Biol. 1753:63–71. [PubMed: 29564781]

Hu C, Fan L, Cen P, Chen E, Jiang Z, and Li L 2016 Energy Metabolism Plays a Critical Role in Stem Cell Maintenance and Differentiation. Int J Mol Sci. 17:253. [PubMed: 26901195]

Idelson M, Alper R, Obolensky A, Ben-Shushan E, Hemo I, Yachimovich-Cohen N, Khaner H, Smith Y, Wiser O, Gropp M, Cohen MA, Even-Ram S, Berman-Zaken Y, Matzrafi L, Rechavi G, Banin E, and Reubinoff B 2009 Directed differentiation of human embryonic stem cells into functional retinal pigment epithelium cells. Cell Stem Cell. 5:396–408. [PubMed: 19796620]

Jang SY, Kang HT, and Hwang ES 2012 Nicotinamide-induced mitophagy: event mediated by high NAD+/NADH ratio and SIRT1 protein activation. J Biol Chem. 287:19304–19314. [PubMed: 22493485]

Jiang M, Esteve-Rudd J, Lopes VS, Diemer T, Lillo C, Rump A, and Williams DS 2015 Microtubule motors transport phagosomes in the RPE, and lack of KLC1 leads to AMDlike pathogenesis. J Cell Biol. 210:595–611. [PubMed: 26261180]

Kim YH, He S, Kase S, Kitamura M, Ryan SJ, and Hinton DR 2009 Regulated secretion of complement factor H by RPE and its role in RPE migration. Graefes Arch Clin Exp Ophthalmol. 247:651–659. [PubMed: 19214553]

Kuznetsova AV, Kurinov AM, and Aleksandrova MA 2014 Cell models to study regulation of cell transformation in pathologies of retinal pigment epithelium. J Ophthalmol. 2014:801787. [PubMed: 25177495]

Maruotti J, Sripathi SR, Bharti K, Fuller J, Wahlin KJ, Ranganathan V, Sluch VM, Berlinicke CA, Davis J, Kim C, Zhao L, Wan J, Qian J, Corneo B, Temple S, Dubey R, Olenyuk BZ, Bhutto I, Lutty G, and Zack DJ 2015 Small-molecule-directed, efficient generation of retinal pigment epithelium from human pluripotent stem cells. Proc Natl Acad Sci U S A. 112:10950–10955. [PubMed: 26269569]

McLaren MJ 1996 Kinetics of rod outer segment phagocytosis by cultured retinal pigment epithelial cells: Relationship to cell morphology. IOVS. 37:1213–1224.

Miceli MV, Newsome DA, and Tate DJ 1997 Vitronectin is responsible for serum-stimulated uptake of rod outer segments by cultured retinal pigment epithelial cells. IOVS. 38:1588–1597.

Mitchell SJ, Bernier M, Aon MA, Cortassa S, Kim EY, Fang EF, Palacios HH, Ali A, Navas-Enamorado I, Di Francesco A, Kaiser TA, Waltz TB, Zhang N, Ellis JL, Elliott PJ, Frederick DW, Bohr VA, Schmidt MS, Brenner C, Sinclair DA, Sauve AA, Baur JA, and de Cabo R 2018 Nicotinamide Improves Aspects of Healthspan, but Not Lifespan, in Mice. Cell Metab. 27:667–676 e664. [PubMed: 29514072]

Musch A 2004 Microtubule organization and function in epithelial cells. Traffic. 5:1–9. [PubMed: 14675420]

Rhyu DY, Yang Y, Ha H, Lee GT, Song JS, Uh ST, and Lee HB 2005 Role of reactive oxygen species in TGF-beta1-induced mitogen-activated protein kinase activation and epithelial-mesenchymal transition in renal tubular epithelial cells. J Am Soc Nephrol. 16:667–675. [PubMed: 15677311]

Rodriguez-Boulan E, and Macara IG 2014 Organization and execution of the epithelial polarity programme. Nat Rev Mol Cell Biol. 15:225–242. [PubMed: 24651541]

Saini JS, Corneo B, Miller JD, Kiehl TR, Wang Q, Boles NC, Blenkinsop TA, Stern JH, and Temple S 2017 Nicotinamide Ameliorates Disease Phenotypes in a Human iPSC Model of Age-Related Macular Degeneration. Cell Stem Cell. 20:1–13. [PubMed: 28061348]

Shyh-Chang N, Daley GQ, and Cantley LC 2013 Stem cell metabolism in tissue development and aging. Development. 140:2535–2547. [PubMed: 23715547]

Singh R, Phillips MJ, Kuai D, Meyer J, Martin JM, Smith MA, Perez ET, Shen W, Wallace KA, Capowski EE, Wright LS, and Gamm DM 2013 Functional analysis of serially expanded human iPS cell-derived RPE cultures. Investigative ophthalmology & visual science. 54:6767–6778. [PubMed: 24030465]

Strauss O 2005 The retinal pigment epithelium in visual function. Physiol Rev. 85:845–881. [PubMed: 15987797]

Tombran-Tink J, Shivaram SM, Chader GJ, Johnson LV, and Bok D 1995 Expression, secretion, and age-related downregulation of pigment epithelium-derived factor, a serpin with neurotrophic activity. J Neurosci. 15:4992–5003. [PubMed: 7623128]

Wang Z, Li Y, and Sarkar FH 2010 Signaling mechanism(S) of reactive oxygen species in epithelial-mesenchymal transition reminiscent of cancer stem cells in tumor progression. Curr Stem Cell Res Ther. 5:74–80. [PubMed: 19951255]

Wavre-Shapton ST, Meschede IP, Seabra MC, and Futter CE 2014 Phagosome maturation during endosome interaction revealed by partial rhodopsin processing in retinal pigment epithelium. J Cell Sci. 127:3852–3861. [PubMed: 25074813]

Wenzel A, Oberhauser V, Pugh EN Jr., Lamb TD, Grimm C, Samardzija M, Fahl E, Seeliger MW, Reme CE, and von Lintig J 2005 The retinal G protein-coupled receptor (RGR) enhances isomerohydrolase activity independent of light. J Biol Chem. 280:29874–29884. [PubMed: 15961402]

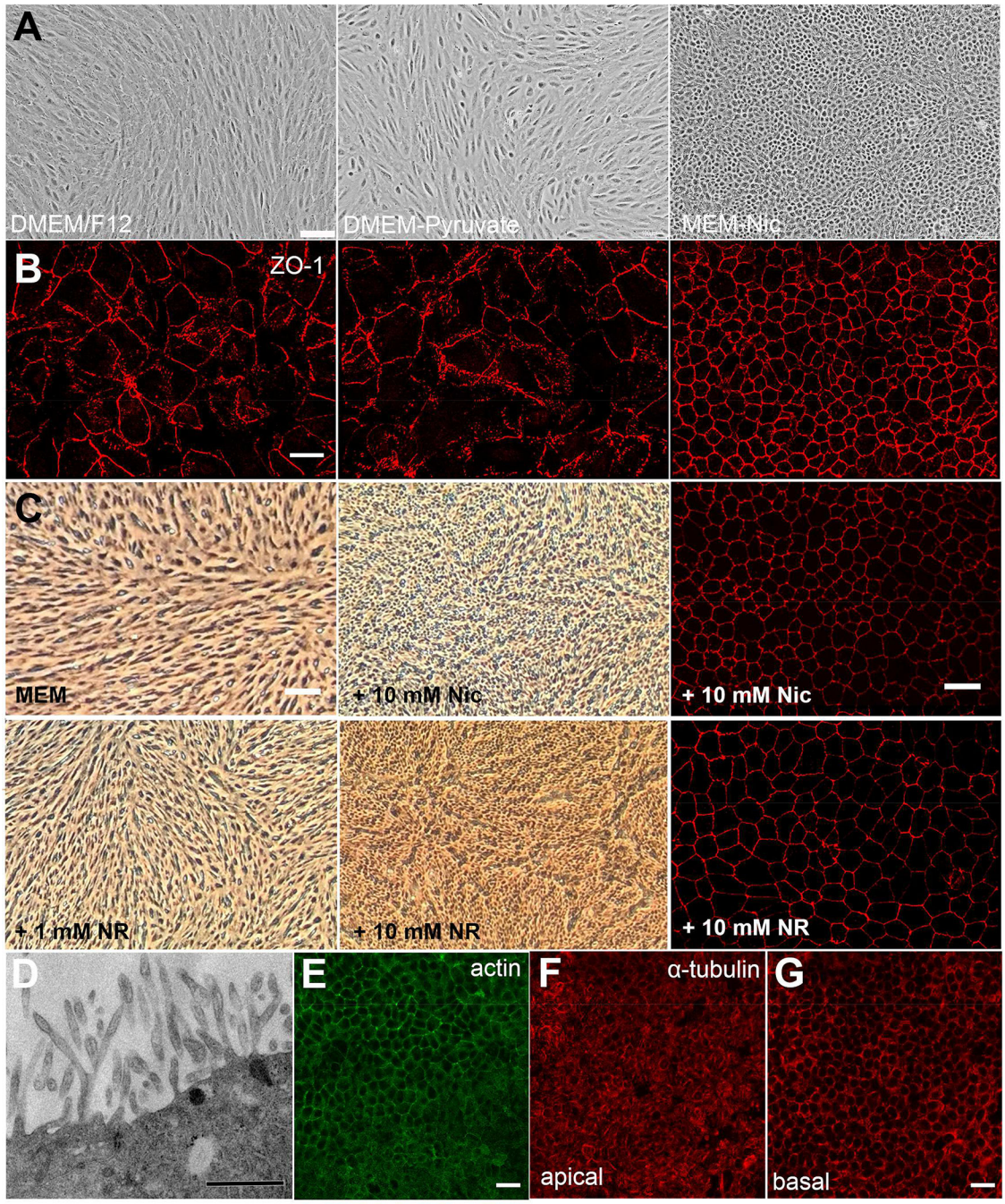

Figure 1: Cellular morphology of differentiated ARPE-19 cells.

(**A**) Brightfield micrographs of ARPE-19 cells differentiated on plastic surfaces for one week in standard media (DMEM/F12 or DMEM-Pyruvate) or in MEM-Nic medium. (**B**) Immunofluorescence micrographs of ZO-1 labeling in ARPE-19 cells differentiated on Transwell inserts for one week in the same media as for **A**. Only cells differentiated in MEM-Nic medium show a cobblestone morphology after this one-week interval. (**C**) Nicotinamide is a necessary component in MEM-Nic for the differentiation of ARPE-19 cells. Brightfield micrographs of ARPE-19 cells plated at the same density and cultured on

plastic tissue culture plates for two weeks in MEM-Nic medium with all supplements, except the nicotinamide, with 1 mM or 10 mM NR instead of the nicotinamide, or with 10 mM nicotinamide (i.e. complete MEM-Nic). Cobblestone morphology can only be observed in medium containing 10 mM Nic or 10 mM NR. The adjacent immunofluorescence images show ZO-1 labeling, after culture on Transwell inserts in MEM plus 10 mM Nic or 10 mM NR for two weeks. Note that different imaging systems were used for the brightfield images in **A** and **C**. NR, nicotinamide riboside. (**D-G**) ARPE-19 cells differentiated on Transwell inserts for 23 weeks in MEM-Nic medium. (**D**) TEM micrograph showing numerous microvilli emanating from the apical surface of ARPE-19 cells. (**E**) Phalloidin labeling showing actin filaments in the apical microvilli (lower) and in a circumferential ring at the level of the cell-cell junctions (upper). (**F and G**) Single plane confocal microscopy of α-tubulin immunolabeling, revealing horizontal microtubules in the apical part of the cell body (**F**) and vertical microtubules in the basal region (**G**) of polarized ARPE-19 cells. Scale bars, 100 μm (**A and C**), 20 μm (**B, E, and G**), or 0.5 μm (**D**). All images are representative from at least 3 experiments.

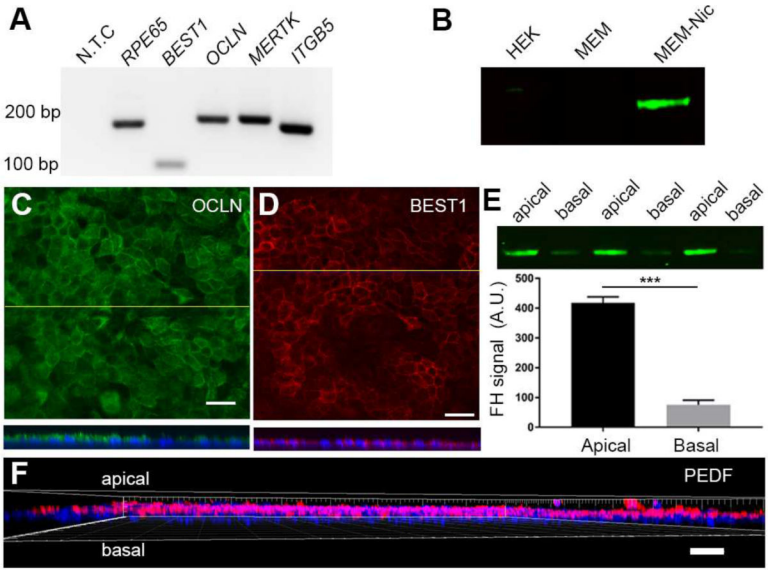

Figure 2: Expression profile and functional assessment of differentiated ARPE-19 cells.

(**A**) RTPCR shows expression of RPE-specific and RPE-related genes. N.T.C, no template control. (**B**) Immunolabeled western blot revealing expression of RPE65 in ARPE-19 cells differentiated in MEM-Nic for 4 weeks; the protein is undetectable in HEK cells and ARPE-19 cells differentiated in MEM without nicotinamide (MEM). See Supplementary Fig. 2A for images of the complete western blot after, first, Ponceau S-staining and, then, immunolabeling. HEK, human embryonic kidney cells. (**C and D**) Fluorescence micrographs of ARPE-19 cells differentiated on Transwell inserts for 3 weeks showing expression and polarized localization of OCLN, at the level of the junctional complexes (**C**), and BEST1, along the basolateral surface (**D**). The nuclei are counterstained with DAPI in the z-planes (taken at the yellow lines), which are shown beneath each panel. Although reconstructed z-axis resolution is considerably inferior to x- and y-axis resolution, creating significant vertical “blur”, it is evident that the OCLN labeling is more apical than the BEST1 labeling, indicating that the BEST1 labeling is below the junctional complex and in the lateral membrane that is part of the basolateral domain. (**E**) Immunolabeled western blot revealing the presence of Factor H in serum-free medium conditioned by differentiated ARPE-19 cells for 48 h. Quantification of band intensity showed significantly more Factor H present in the apical medium relative to the basal medium. Samples from three different cultures (n = 3) are shown; for each pair, the volume of basal medium loaded on to the gel was 6 times larger than the volume of apical medium in order to account for the difference in medium volume placed in the apical and basal chambers of the Transwell insert. See Supplementary Fig. 2B for image of complete western blot. (**F**) Z-projection of fluorescence micrograph of differentiated ARPE-19 cells showing expression and apical localization of PEDF, a protein secreted from the apical surface of polarized RPE cells. Scale bars, 20 μm (**C, D, F**). PEDF, pigment epithelium-derived factor. All images are representative of ≥ 3 experiments. Error bars in (**E**) represent ± S.E.M. *** $P = 0.0002$.

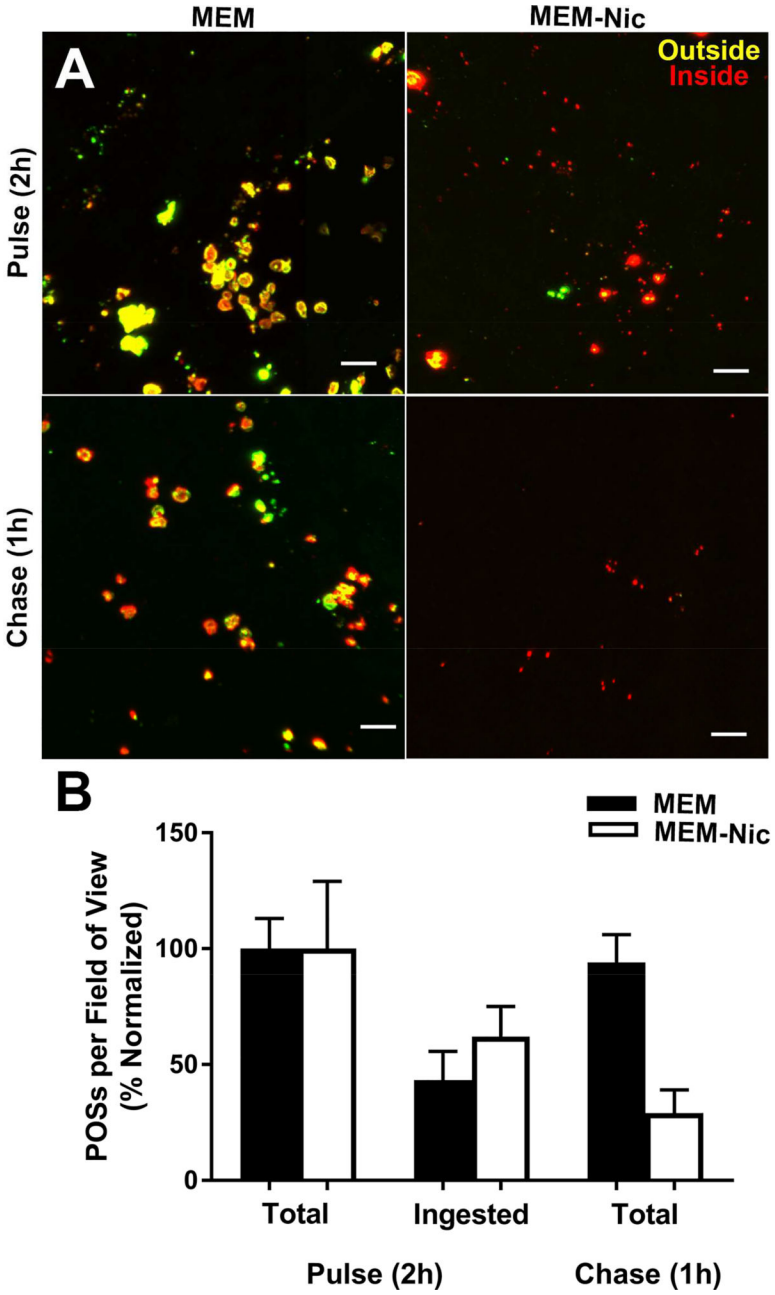

Figure 3: Phagocytic function in differentiated ARPE-19 cells.

(**A**) Micrographs of opsin-labeled ARPE-19 cells (before and after cell permeabilization) cultured on Transwell inserts in MEM or MEM-Nic, following exposure to porcine POSs for 2 h and fixed immediately (pulse), or fixed after a further 1-h chase period in the absence of POSs. Surface-bound POSs appear in yellow whereas internalized POSs appear in red. (**B**) Bar graph showing quantification of POSs. Data were normalized relative to the total number of POSs (bound and ingested) after the pulse (n = 7 fields of view, aggregated from separate experiments). The relative number of ingested POSs (i.e. POS phagosomes) after

the pulse (n = 4) and the total number of POSs after the chase (n = 7) are also shown. Scale bar, 10 μm. Error bars in (**B**) represent ± S.E.M. Each field of view (n) contained ≥ 100 cells.